An instrument for precise measurement of viscoelastic properties of low viscosity dilute macromolecular solutions at frequencies from 20 to 500 kHz

Theodore M. Stokich,[a] Douglas R. Radtke,[b] Christopher C. White, and John L. Schrag

Department of Chemistry and Rheology Research Center, University of Wisconsin, Madison, Wisconsin 53706

(Received 16 November 1993; accepted 26 February 1994)

Synopsis

A high-frequency torsional rod apparatus (HFTRA) has been developed for measurements of moderately high-frequency viscoelastic properties of dilute, low viscosity polymer solutions. It employs a long cylindrically shaped resonating element driven by an X-cut (torsional mode) quartz piezoelectric crystal. Up to 11 different normal modes are employed, resulting in 11 discrete frequencies, ranging from approximately 20 to 500 kHz. Measurements are made in free decay; a key feature of the apparatus is the method for high precision measurements of damping coefficients and eigenfrequencies. The instrument is suitable for liquids with $0.003P < |\eta^*| < 5P$ and $\eta' \geq 1.33\eta''$. Typically, η' has a relative uncertainty of $\pm 2\%$ or less, with the relative uncertainty for η'' being about 4% for liquids with η'' greater than $0.01P$. Values of η' obtained in the HFTRA for low viscosity liquids with small η'' show excellent agreement with the known steady flow viscosities. Measurements of the viscoelastic properties of polymer solutions employing the HFTRA and two other instruments capable of higher precision measurements show excellent agreement, demonstrating that the HFTRA is sufficiently precise for dilute-solution viscoelasticity studies; the working frequency range is such that most of the polymer relaxation time spectrum can be probed for many polymer/solvent combinations.

I. INTRODUCTION

Extensive studies of the linear viscoelastic properties of polymer solutions have provided considerable insight into the dynamics of conformational change in both the dilute and semidilute regimes [Ferry (1980)]. To investigate chain dynamics by means of linear viscoelastic properties, it is necessary to employ instrumentation operating at frequencies capable of probing at least a major fraction of the relaxation time spectrum of the polymer. Table I lists the longest and shortest relaxation times observed for a dilute solution of a narrow-distribution 860 000 MW polystyrene in a solvent which exhibits widely differing viscosities at different temperatures. Also listed are experimental time scales reported in terms of corresponding shearing frequency ranges necessary to probe the entire range of conformational dynamics exhibited by this particular polymer–solvent combination. In order to adequately explore the relaxation time spectrum of a polymer in a dilute solution via linear viscoelasticity, it is essential to obtain high precision measure-

[a]Present address: Dow Chemical Co., Central Research, 1712 Building, Midland, Michigan 48674.
[b]Present address: Rhône-Poulenc Inc., CN 7500, Cranbury, New Jersey 08512.

TABLE I. Temperature dependence of the longest and shortest relaxation times observed for a 0.0040 g/cm^3 solution of 860 000 MW polystyrene in Aroclor 1248.

Approximate solution viscosity (P)	Temp (°C)	Longest relaxation time[a] (s)	Shortest relaxation time[b] (s)	Instrumental frequency range[c] (Hz)
0.7	45.00	1.4×10^{-3}	3×10^{-7}	20 Hz–2 MHz
4	25.00	9×10^{-3}	2×10^{-6}	4 Hz–300 kHz
350	2.80	0.75	2×10^{-4}	4×10^{-2}–3000 Hz
1 200	−1.40	3	6×10^{-4}	1×10^{-2}–1000 Hz
8 000	−4.00	19	4×10^{-3}	2×10^{-3}–150 Hz
25 000	−10.00	56	1×10^{-2}	6×10^{-4}–60 Hz

[a]Data of Landry [Landry (1985)].
[b]Data of Landry and Sammler [Landry (1985); Sammler (1990)].
[c]Instrumental frequency range required to explore the entire relaxation time spectrum.

ments; results are generally reported in terms of the real and imaginary parts of the complex shear modulus, $G^*(G^* = G' + iG'' = G_m e^{+i\delta})$, or those of the complex viscosity coefficient, $\eta^*(\eta^* = \eta' - i\eta'' = \eta_m e^{-i\phi})$.

Instruments for high precision viscoelasticity measurements for dilute polymer solutions employ steady-state, very small strain, simple shearing flows. Commercial instruments employing cone-and-plate or parallel-plate geometries typically have an upper frequency limit of about 40–100 Hz (and generally do not have adequate precision), which is not nearly high enough to explore the entire relaxation time spectra for typical dilute polymer solutions, as is illustrated in Table I, unless a very high viscosity solvent is employed. Such a solvent usually requires a wide instrumental working temperature range and excellent (0.002 °C) temperature control. Custom instrumentation, such as the modified Birnboim Apparatus (MBA), which employs the Segel–Pochettino or annular pumping geometries, has substantially broader frequency ranges; the MBA is useful from 0.001 to 1000 Hz for moderate to high viscosity samples ($|\eta^*| \geq 5P$). These instrumental frequency range limitations can often be circumvented by employing time–temperature superposition [Ferry (1980)] for solutions employing good solvents which exhibit a strong dependence of viscosity on temperature. However, this requires good solvent conditions at every temperature to avoid chain radius of gyration changes. By making measurements at several different temperatures, the relaxation time spectrum $\{\tau_p\}$ of the polymer can be shifted in time without altering the relaxation time *ratios* $\{\tau_p/\tau_1\}$. This approach has been used with the MBA to cover an *effective* frequency range of 10^{-5}–10^6 Hz, which is sufficient to explore the entire relaxation time spectrum of the polymer solution of Table I. However, the need to employ time–temperature superposition imposes two significant restraints (noted above) upon the polymer–solvent systems that can be studied. First, the solvent must be a good solvent for the polymer at *all* measurement temperatures, and second, the solvent viscosity must be strongly temperature dependent. This greatly restricts the solvents that may be employed in such studies. Thus the relaxation time spectra of solutions in solvents such as water (most biological systems), toluene, dioctyl phthalate, or hexane could be explored only to a very limited extent. Thus, it is necessary to have instrumentation that is capable of both adequate precision and a large actual shearing frequency range, ideally extending up to about 10^7 Hz, in order to fully explore chain dynamics in polymer solutions employing such low viscosity solvents.

Several different instrumental strategies have been employed to measure linear viscoelastic properties of solutions based on low viscosity solvents. What follows is a brief description of the major types of instruments developed to date. A more complete listing has been given by Ferry [Ferry (1980)].

An instrument operating in the low- to mid-audio frequency range was developed by Sittel, Rouse, and Bailey [Sittel (1954)] and later modified by Mellema [Blom (1984)]; it was based on a hollow torsional pendulum geometry and had an operating frequency range from 80 to 2500 Hz. The instrument of Sittel was operated in torsional free decay (TFD), and the eigenfrequency and damping coefficient were measured. Mellema improved the precision of this method by using forced oscillations. In both cases, a different pendulum was required for each frequency studied.

The Multiple Lumped Resonator (MLR), first suggested by Birnboim [Ferry (1980)], was developed by Johnson and Schrag [Schrag (1972)] and later modified by the Amis group [Hair (1989)] and the Elgsaeter group [Ellingsrud (1992); Mikkelsen (1992)]. This instrument incorporates a resonator machined from a single piece of high-Q metal, which consists of five lumps connected by small diameter sections (springs) with different radii. This geometry creates five measurement frequencies (resonance modes), typically between 100 and 8000 Hz; the MLR is capable of very high measurement precision, but the 8000 Hz maximum shearing frequency is far less than what is needed to explore the short time end of the relaxation time spectrum of the low viscosity solutions for which it is designed ($|\eta^*| < 0.3P$).

The use of a piezoelectric quartz tuning fork with wide, thin oscillating arms was pioneered by Mason [Mason (1947)] and has been employed by Yoshizaki [Yoshizaki (1993)]. For every frequency measured, a separate tuning fork is employed. The reported working frequency range is 0.5–10 kHz.

Glover [Glover (1968); Glover (1969)] was the first to employ a thin hollow nickel tube transducer in which a traveling torsional wave packet induced by magnetostriction gave rise to cylindrical shear waves propagating in the surrounding liquid. The advantage of this instrument was that it was not restricted to specific frequencies, although the resultant measurement precision was poor. This basic design was improved on by Cooke and Matheson [Cooke (1976)], and later modified by Oosterbroek and Mellema [Oosterbroek (1980)] for use in a steady-state mode, which restricted measurements to discrete resonance frequencies (fundamental and five overtones), but substantially increased measurement precision. The demonstrated frequency range was 11–200 kHz.

Cylindrical torsional mode piezoelectric crystals were first employed by Mason [Mason (1947)] for electrically nonconductive solutions. A different crystal was employed for each shearing frequency; the discrete frequency range covered was 20–100 kHz. This approach was improved upon by Tanaka and Sakanishi [Tanaka (1966)], who employed phase-sensitive detection to increase measurement precision. McSkimin attached a quartz buffer rod to the bottom of a quartz crystal, which gave rise to a set of additional lower-frequency modes, and enabled measurements on electrically conducting solutions [McSkimin (1952)]. The Wada group [Nakajima (1973); Nakajima (1970)] employed the torsional-free decay (TFD) method and a McSkimin-type resonator. This approach extended the lower end of the working frequency range to 2 kHz (the working range of the instrument was 2–20 kHz); later, the Wada group extended the frequency range to higher frequencies (six frequencies between 2.2 and 525 kHz) [Ookubo (1976)].

The use an aluminum plate delay line in which a piezoelectrically generated ultrasonic transverse wave (Meitzler mode) was used to generate steady-state shear wave propagation in the liquid sample was pioneered by the Meitzler group [Meeker (1964)] and modified by Hunston [Hunston (1969); Hunston (1972)]. A working frequency range of

1–7 MHz was achieved. The Birnboim group [Koh (1977)] further modified this technique, employing fused quartz for the delay lines, which extended the frequency range to higher frequencies (3–30 MHz).

For still higher frequencies, instruments have been developed in which piezoelectrically generated shear waves propagate through quartz, and are modified by reflection at an interface between the quartz and the viscoelastic liquid being studied. This method was initially employed by the Mason group [Mason (1949)] and had a frequency range of 3–100 MHz. This scheme was modified extensively by Lamb and co-workers [Barlow (1959)], which resulted in a major expansion of the frequency range (40–1500 MHz).

All the above instruments, with the exception of that of the Wada group, measure the motional differences of the resonator with and without contact with the viscoelastic liquid. An important advantage of the approach taken by the Wada group is that TFD measurements employing a long resonator geometry of the McSkimin type enable several measurements for each mode at different depths of immersion in the polymer solution, so that it is not necessary to make measurements with no sample present. More importantly, this measurement scheme greatly reduces the scatter in the measured properties. This approach is possible with most of the geometries listed above, with the exception of the plate delay line resonators and flat crystals, but it has not been employed because of complications introduced by solution surface wave effects.

In the development of the high-frequency instrumental strategies outlined above, the advantage of a continuous frequency capability obtained when employing torsional traveling wave packets was offset by poorer measurement precision. On the other hand, measurements at resonance frequencies (steady-state or TFD methods) had the disadvantage of a restricted set of frequencies but had substantially enhanced measurement precision. With the focus of the instrument described here being adequate precision for dilute solution studies, the TFD method has been employed. The apparatus is a variation on the Wada instrument; the major differences lie in the detection schemes. His scheme employed analog electronics while our approach uses a combination of digital and analog methods to substantially improve the precision of the measurement.

II. DESCRIPTION OF RESONATOR

The type of resonator employed in this instrument was first described by McSkimin [McSkimin (1952)]; it is shown diagrammatically in Fig. 1. The cylindrically shaped resonator element is composed of an 0.500 cm diameter Homisil fused quartz rod (Heraeus–Amersil) 76.333±0.002 cm in length, bonded to a 10.000±0.002 cm X-cut (torsional mode) quartz piezoelectric crystal with plated gold electrodes, manufactured by Valpey–Fisher, also 0.500 cm in diameter. The two pieces of the resonator are fastened together using Norland Optical Adhesive #61; a very thin glue layer is essential so that the mechanical impedance of the layer does not result in unwanted alterations of the standing wave patterns at high frequency. The electrical contacts to, and lateral stability for, the resonator are accomplished by four orthogonally placed phosphor–bronze electrodes, sharpened to a fine edge, contacting the vertical center of the piezoelectric crystal, as shown in Fig. 2. This vertical center corresponds to a node for all of the modes employed. A small (0.05 cm diam, 0.05 cm deep) conically shaped indentation in the center of the bottom of the quartz rod facilitates positioning of the resonator inside the housing. The resonator rests on a titanium support pin with a very sharp point to minimize the influence of this contact on the motion of the resonator. The vertical positioning of the resonator within the housing is accomplished by raising or lowering the support pin. A fine vertical positioning capability is essential: In practice, the electrodes must

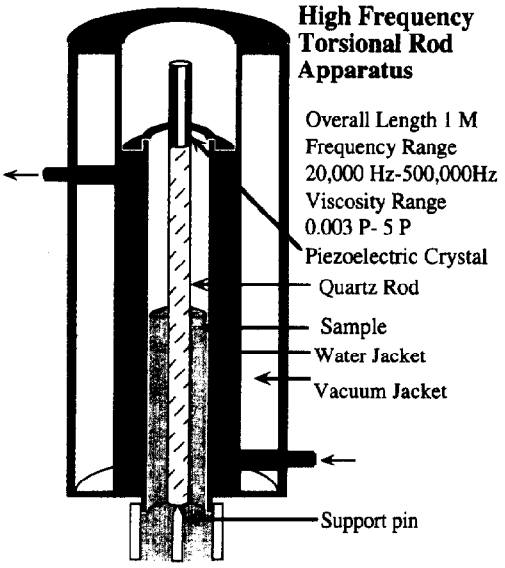

FIG. 1. Schematic diagram of the resonator and housing for the high frequency torsional rod apparatus (not to scale).

contact the resonator within ± 0.001 in. of its vertical center. If the contact point is in error by ± 0.005 in., the resultant damping of the rod motion completely masks that caused by the sample solution. It is important to note that the length of the fused quartz buffer rod is not an integer multiple of the physical length of the piezoelectric crystal; the velocity of propagation of torsional shear waves is smaller in the fused quartz rod than in the piezoelectric crystal quartz driver element. To correct for this difference the fused quartz rod was shortened by 3.667 cm, so that the buffer rod would have an *effective* length (units of wavelength) that is an integer multiple of the length of the piezoelectric

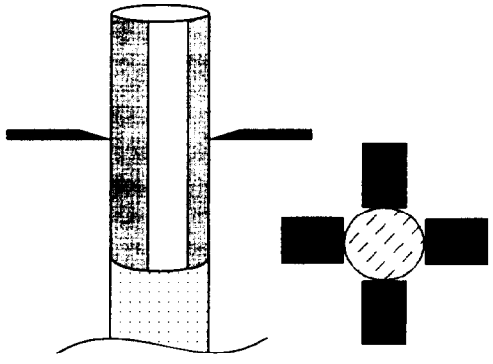

FIG. 2. Placement of the electrodes on the cylindrical torsional mode drive crystal (top and side view). Oppositely placed electrodes are electrically connected.

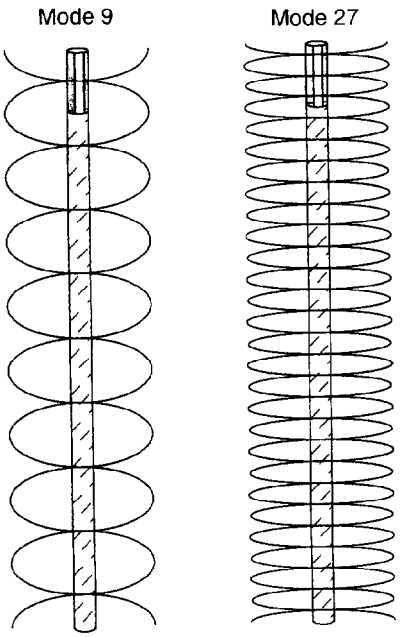

FIG. 3. Visualization of the envelope of standing wave patterns of the resonator motion for the two lowest modes currently employed. The two ends of the rod and the junction between the torsional crystal and the buffer rod are antinodes, and the point of electrode contact is at a node.

crystal. In order to obtain sufficiently large motional amplitudes to be readily detected, it is necessary to drive the resonator at a normal mode (resonance) frequency before the torsional-free decay process begins. For all normal modes, there is an antinode at each end of the resonator. In addition, there must be a node at the point of contact between the electrodes and the resonator to avoid excessive damping of the resonator due to these contacts, and there should also be an antinode at the glued junction between the two elements to minimize the influence of the glue layer. These constraints lead to eleven usable frequencies in the range $19 < f < 500$ kHz for the resonator dimensions listed above. From these, usually eight are chosen that are approximately evenly spaced along a log frequency axis. The eight modes (frequencies) currently employed are modes 9 (19 640 Hz), 27 (59 979 Hz), 45 (98 360 Hz), 63 (137 695 Hz), 81 (177 085 Hz), 117 (255 857 Hz), 153 (334 693 Hz), and 208 (455 078 Hz).

The spatially and temporally varying angular displacement of the resonator is generated by the application to the electrodes of a sinusoidally time varying voltage of precisely controlled (1 part in 10^9) frequency. This produces torsional plane shear waves that propagate up and down in the composite resonator, reflecting from its top and bottom, which results in standing wave patterns, as are depicted in Fig. 3 for the first two normal modes currently employed.

The angular displacements of the resonator surface produce cylindrical shear waves propagating out radially in the surrounding medium. The working equations employed assume that these shear waves are effectively spatially attenuated to zero ["surface loading condition;" Ferry (1980)] before they encounter the glass sample cell wall (0.15 cm

gap between the resonator and the wall). A purely viscous sample ($\eta'' = 0$) would violate this condition for $|\eta^*| > 12P$; for a fairly elastic sample ($\eta' = 1.33\eta''$), this condition would be violated at $|\eta^*| > 7P$. This criterion is a major factor in determining the high viscosity limit for the instrument.

While the resonator is being driven, only some of the applied electrical energy is translated into mechanical energy by the piezoelectric effect of the crystal, which complicates the analysis of steady-state measurements. For this reason, all measurements are taken when the resonator is in torsional free decay (TFD).

To generate the free decay signal, the resonator is first driven at a normal mode (resonance) frequency long enough to develop a steady-state standing torsional shear wave in the resonator. Next, the drive electronics are turned off, and the subsequent torsional free decay of the driver motion is monitored by measuring the piezoelectrically generated voltage (V_T) appearing at the phosphor–bronze electrodes,

$$V_T = V_M^T e^{(-t/\tau)} \sin(\omega_{en} t + \delta), \tag{1}$$

where V_M^T is the magnitude, ω_{en} (rad/s) is the radian eigenfrequency for mode n, and $1/\tau$ (s^{-1}) is the damping factor.

To obtain the viscoelastic properties of the solution, working equations relating $\Delta(1/\tau)$, $\Delta\omega_{en}$, and the solution η^* are necessary. The working equations employed are those of Wada [Nakajima (1973)], which were derived by employing a transmission line analogy. He obtained

$$\Delta\left(\frac{1}{\tau}\right)_n = \left([(\eta'^2+\eta''^2)^{1/2}+\eta'']\frac{\omega_{en}\rho}{2}\right)^{1/2}\left(\frac{2h}{\rho_0 a l}\right)\left[1+\frac{l}{2n\pi h}\sin\left(\frac{2n\pi h}{l}\right)\right] \tag{2}$$

and

$$\Delta\omega_{en} = -\left([(\eta'^2+\eta''^2)^{1/2}-\eta'']\frac{\omega_{en}\rho}{2}\right)^{1/2}\left(\frac{2h}{\rho_0 a l}\right)\left[1+\frac{l}{2n\pi h}\sin\left(\frac{2n\pi h}{l}\right)\right] \tag{3}$$

for mode n, where η', η'', and ρ are the real and imaginary components of the complex viscosity coefficient for the solution and the density of the solution, respectively; ω_{en} is the eigenfrequency of the resonator; and ρ_0, a, l, and h are the density, radius, length, and depth of immersion for the cylindrical resonator, respectively. There are two terms containing the dependence of $\Delta(1/\tau)$ and $\Delta\omega_{en}$ on the depth of immersion: a linear term and a sinusoidal term that is mode dependent. The inverse mode number dependence of the sinusoidal term reduces its influence as n increases; in practice, the contribution from the sinusoidal term is smaller than experimental noise for mode numbers greater than 20.

Equations (2) and (3) can be expressed in terms of an instrumental constant K and the real and imaginary terms of the characteristic impedance $Z^s_{m,\mathrm{pl}}$ for plane shear waves ($Z^s_{m,\mathrm{pl}} = R^s_{m,\mathrm{pl}} + iX^s_{m,\mathrm{pl}}$):

$$\Delta(1/\tau)_n \cong KR^s_{m,\mathrm{pl}} \tag{4}$$

$$\Delta\omega_{en} \cong -KX^s_{m,\mathrm{pl}} \tag{5}$$

where the $R^s_{m,\mathrm{pl}}$ and $X^s_{m,\mathrm{pl}}$ are [Schrag (1971)]

$$R^s_{m,\mathrm{pl}} = \sqrt{\omega\rho\eta_m}\cos\left(\frac{\varphi}{2}-\frac{\pi}{4}\right) = \left(\frac{\omega\rho}{2}[(\eta'^2+\eta''^2)^{1/2}+\eta'']\right)^{1/2}, \tag{6}$$

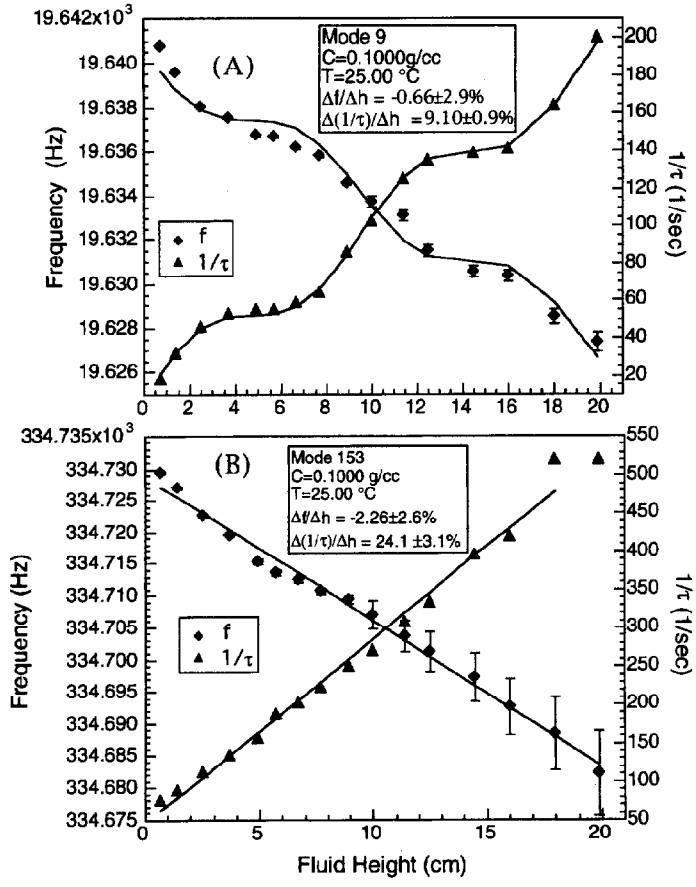

FIG. 4. Plots of eigenfrequency and damping coefficient versus fluid height for 0.100 g/cm^3 solution of polyisoprene in cis-decalin. (Error bars on the eigenfrequency reflect the 95% confidence interval.) Lines are best fit lines using Eq. (8) (line slopes and uncertainties are also listed). (a) Mode 9 (19 640 Hz). (b) The same plot for mode 153 (334 720 Hz).

$$X^s_{m,\mathrm{pl}} = -\sqrt{\omega\rho\eta_m}\,\sin\left(\frac{\varphi}{2}-\frac{\pi}{4}\right) = \left(\frac{\omega\rho}{2}[(\eta'^2+\eta''^2)^{1/2}-\eta'']\right)^{1/2}, \tag{7}$$

and K is

$$K = \frac{2h}{\rho_0 a l}\left[1+\frac{l}{2n\pi h}\sin\left(\frac{2n\pi h}{l}\right)\right]. \tag{8}$$

Figure 4 illustrates the agreement between the predictions of Eqs. (4), (5), and (8) and experimental data. In Fig. 4(a), the solid lines represent a best fit to the data; the best fit constants are essentially identical to those predicted from the measured physical dimensions of the resonator. The directly measured length of the composite resonator is 86.333 cm (±0.002), which gives 1.5267 cm (±0.002%) for $l/(2n\pi)$; the theoretical best fit to the experimental data gives 1.513 cm (±0.7%). Figure 4(b) shows the fit for a higher

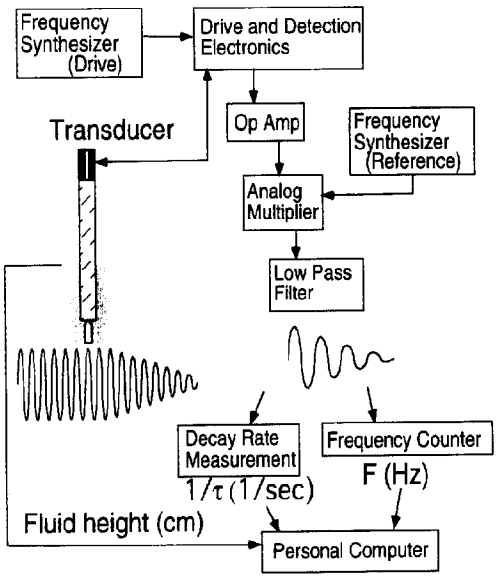

FIG. 5. Diagram of the HFTRA measurement scheme. The motion of the transducer is illustrated; only the free decay portion is sensed in the detection scheme.

mode number; note that $1/\tau$ and ω_{en} show the linear dependence on fluid height seen for mode numbers greater than 20.

The η' and η'' are obtained by rearrangement of Eqs. (4) and (5).

$$\eta' = \frac{2R^s_{m,\mathrm{pl}}X^s_{m,\mathrm{pl}}}{\omega\rho} = \frac{-2(\Delta\omega)_{en}(\Delta 1/\tau)_n}{\omega_{en}\rho K^2} \tag{9}$$

$$\eta'' = \frac{R^{s2}_m - X^{s2}_m}{\omega\rho} = \frac{(\Delta 1/\tau)^2_n - (\Delta\omega)^2_{en}}{\omega_{en}\rho K^2} \tag{10}$$

III. IMPLEMENTATION OF MEASUREMENT SCHEME

In order to measure the viscoelastic properties of dilute polymer solutions with enough precision to extract the polymer contribution, high precision measurements of $1/\tau$ and ω_{en} are essential. In practice, precisions of greater than 1 part in 10^6 are required for both the frequency and damping factor measurements to determine the viscoelastic properties with a relative precision of 1%.

An outline of the measurement scheme is shown in Fig. 5. First, the resonator is driven at a resonance frequency (ω_{res}) by applying a sinusoidally time varying voltage from a Hewlett-Packard model 3325A frequency synthesizer equipped with the high-stability 10 MHz master clock option (frequency stability better than 1 part in 10^9 for the time intervals involved). When the resonator has reached steady-state conditions, the drive signal is gated off by the master timing circuitry. The resonator motion in free decay (TFD) is subsequently followed by monitoring an amplified version of the free decay signal (V_T) generated by the piezoelectric element.

To measure the eigenfrequency with the requisite precision requires the use of a very high-stability universal counter. High-stability counters generally employ special 10 MHz time bases; higher master clock frequencies are generally not sufficiently stable. Such counters operate in either the "frequency" or "period" mode, but adequate precision cannot be obtained for this application when the "frequency" mode is employed, since in this mode the master clock controls the input gate time and the counter counts the number of zero crossings of the incoming transducer signal during the gate interval. Thus, to obtain a precision of 1 part in 10^6, at least 10^6 signal cycles must be counted during the interval. However, the TFD signal decays sufficiently rapidly that there are only about 10^4 cycles before the signal-to-noise ratio approaches unity, making this mode unusable (typical viable measurement times range from 4 to 80 ms). In the "period" mode, the incoming TFD signal sets the gate time interval, and the counter counts the number of zero crossings of the 10 MHz master clock signal during the gate interval. The particular counter employed here, a Hewlett-Packard Model 5328A Universal Counter with the high-stability 10 MHz time base option, has another important feature. In the "period" mode, one can average over more than one period of the incoming waveform; typically, we average over ten cycles. However, even this flexibility will not provide the requisite precision. Consider, for example, the measurement precision obtained for a 100 kHz transducer signal (period = 10^{-5} s) in the period mode; averaging over ten cycles, the measurement precision would be 1 part in 10^3, a long way from the desired 1 part in 10^6.

A heterodyning step is employed to overcome this problem; the transducer signal (V_T) is fed into one channel of an Analog Devices Model 429B multiplier (10 MHz bandwidth). The other input to the multiplier circuit is a high-stability reference sine wave from a second HP3325A frequency synthesizer operating from the same high-stability clock as the drive synthesizer. The frequency of this "offset" signal, ω_0, is set quite close to, but less than, the eigenfrequency of the TFD signal (typically 1000–4000 Hz lower), and has the form

$$V_0 = V_M^0 \sin(\omega_0 t + \gamma). \tag{11}$$

The output of the multiplier ($V_{\text{out}} = V_0 \times V_T$) has the form

$$V_{\text{out}} = V_M^{\text{out}} e^{-(t/\tau)} \left[\sin\left((\omega_{en}+\omega_0)t + \frac{\pi}{2} + \chi\right) + \sin\left((\omega_{en}-\omega_0)t + \frac{\pi}{2} + \chi\right) \right]. \tag{12}$$

Note that frequency sum and difference terms appear, but the damping factor is unchanged. This output is fed to a Krohn–Hite Model 3202 low pass filter; by setting this sharp cutoff filter to transmit only the difference frequency, the filter output has the form

$$V_F = V_M^F e^{-(t/\tau)} \sin[(\omega_{en}-\omega_0)t + \theta]. \tag{13}$$

By heterodyning the signal, the precision in the "period" mode has been enhanced, since the gate time has been increased by of the order of 10^3, so that many more pulses from the master clock are counted. The precision of this measurement for a 1000 Hz difference signal is 1 part in 10^5 (a ten period average). Since the frequency "offset" signal is known to better than one part in 10^9, the actual transducer eigenfrequency (the sum of the "offset" and difference frequencies) can now be measured to better than one part in 10^7 for frequencies above 100 kHz (the last five modes) and one part in 10^6 (the first three modes) for frequencies below 100 kHz.

The heterodyning of the signal also enables the use of a unique method for determination of the damping coefficient of the TFD signal, which was developed by Stokich; this ability to very precisely measure the damping coefficient is the most important aspect

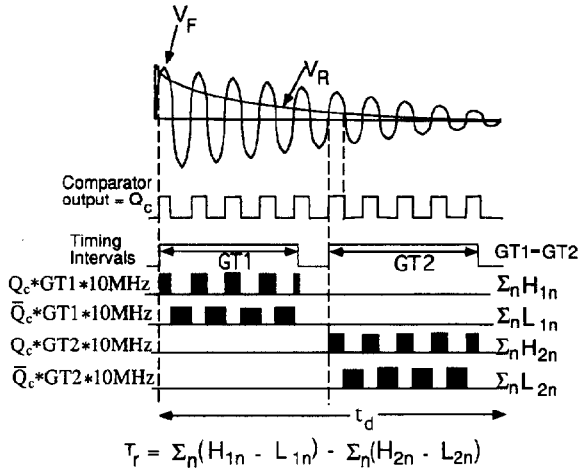

FIG. 6. Outline of the scheme for precise measurement of the damping coefficient of the TFD signal.

of this measurement scheme. The method is illustrated in Fig. 6 (the number of cycles for the V_F signal reduced for clarity). The heterodyned TFD V_F signal is compared to a precise, exponentially decaying reference signal V_R, generated by discharging a high-stability precision 0.1000 μF capacitor through a very low inductance precision decade resistance box. This reference signal has the form

$$V_R = V_M^R e^{-(t/\tau_R)}. \tag{14}$$

The outputs of the very fast comparator and a 10 MHz clock module are fed to the two inputs of digital gating circuitry that feeds a fast synchronous up/down counter; the comparator output state reflects whether $V_F > V_R$, or vice versa. Master control timing circuitry generate the two identical width gates GT1 and GT2 (can be varied from 6.2500×10^{-7} to 0.10000 s). When GT1 and the comparator outputs are both high, the 10 MHz clock signal is fed to the "up" input of the up/down counter; when GT1 is high but the comparator output is low, the 10 MHz signal is fed to the "down" counter input. When GT2 becomes high, the overall operation is reversed, so that when the comparator output is high, the 10 MHz signal is fed to the "down" counter input, and when the comparator output is low, the 10 MHz signal is fed to the "up" input. At the end of the data acquisition interval, t_d, the counter reading reflects the difference in the damping coefficients of V_F and V_R. The damping coefficient of V_R is adjusted by varying the precision decade resistance box setting until V_F and V_R have the same damping coefficient (counter reading is effectively zero). The limiting factors in the determination of the damping coefficient for V_R are the resistance increments of a very low inductance decade resistance box (1 Ω steps) and the noise level of V_F. T_r is averaged up to 2048 times; this is essential to reduce scatter resulting from comparator triggering noise.

There is a small difference between the steady-state resonance frequency of the driven rod and the frequency it has in free decay, the eigenfrequency. Thus, the first several cycles of the decay signal are transitional, not at either of the two frequencies. To keep this from impacting measurements of the eigenfrequency or decay rate (small effect), a precision clock delay circuit is employed that delays the onset of measurement by finite time steps, ranging from 0.1 to 20 milliseconds. During the course of a data run the time

delay is adjusted so that the first several cycles [usually 50–400 cycles of the resonator signal (frequency ω_{en})] of the resonator in free decay are not employed in the eigenfrequency and decay rate measurements.

Temperature control is critical, due to the variation of the eigenfrequencies with temperature. A temperature variation of 0.05 °C produces eigenfrequency changes of as much as 10% of the eigenfrequency shift caused by the viscoelastic liquid, and thus a 10% error in η' and a much larger error in η''. Temperature control is provided by circulating water from a constant temperature bath through passages machined in the housing, as is illustrated in Fig. 1. Additional temperature stability and the reduction of thermal gradients along the resonator are gained by incorporating an outer chamber vacuum jacket as part of the housing. Temperature is measured by three Fenwal GB32P3 thermistors located 1/4, 1/2, and 3/4 of the way up the housing that extend into the bath fluid, and an additional thermistor placed within the bottom support pin. All thermistors have been calibrated against a standard platinum resistance thermometer calibrated at NIST. Changes of ± 0.002 °C can be readily detected. The temperature can be maintained to within ± 0.005 °C for bath temperatures within ± 5 °C of the ambient room temperature; there is no detectable temperature gradient within the cell. Note that a single data run may require up to 15 h.

Measurements are made at several different depths of immersion; depth is controlled by incremental injections of the viscoelastic liquid into the bottom of the sample cell. It is essential to incrementally *fill* the sample cell (successively *increase* the depth of immersion) rather than drain it. If the sample is incrementally drained out of the cell, the thin layer of liquid still coating the resonator strongly affects the eigenfrequency and damping coefficient, and also makes it impossible to accurately determine the effective depth of immersion. This effect persists until the rod is cleaned and dried. Such sensitivity to the presence of a very thin layer of solution suggests that there might be problems when studying liquids with high vapor pressures; vapor deposition of a very thin layer of solvent on the nonimmersed part of the resonator could lead to erroneous results. (The system is essentially sealed to minimize the evaporative loss of sample and deposition of vapors originating from outside the apparatus; for sample liquids such as cyclohexane and toluene, no detectable changes in fluid height or resonance frequencies have been observed during a one hour interval.) The possibility of errors resulting from sample vapor adsorption was explored by monitoring the resonator behavior before and after introducing neat toluene, a relatively high vapor pressure liquid, below the bottom of the resonator, and comparing the resultant frequency and decay rate changes to those observed for neat toluene as a liquid sample. This comparison showed that the toluene vapor adsorbed on the nonimmersed resonator produced no measurable decay rate change, and a very small (< 1 Hz, mode 117) shift in ω_{en}; this would correspond to a *worst case* error of two percent in the measured change in the eigenfrequency and thus less than one percent error in measured properties for toluene; since most solutions have substantially smaller vapor pressure, this is not expected to be a problem. Note that after immersion and drainage (a neat toluene sample), a time interval of at least 20 min was required to evaporate enough of the thin toluene film for the resonator behavior to approach that of the clean resonator. Introduction of the sample into the bottom of the cell is through the hollow support pin. The fluid height, h, is measured by reading the liquid meniscus position on a precise measuring tape attached to the outside of the sample cell; h is measurable to ± 0.01 cm.

The HFTRA working equations [Eqs. (2) and (3)] strictly apply only for long resonators and $h \gg 0$, so that effects associated with the upper liquid surface and the lower end of the resonator are negligible. The lower outer edge and bottom surface of the resonator

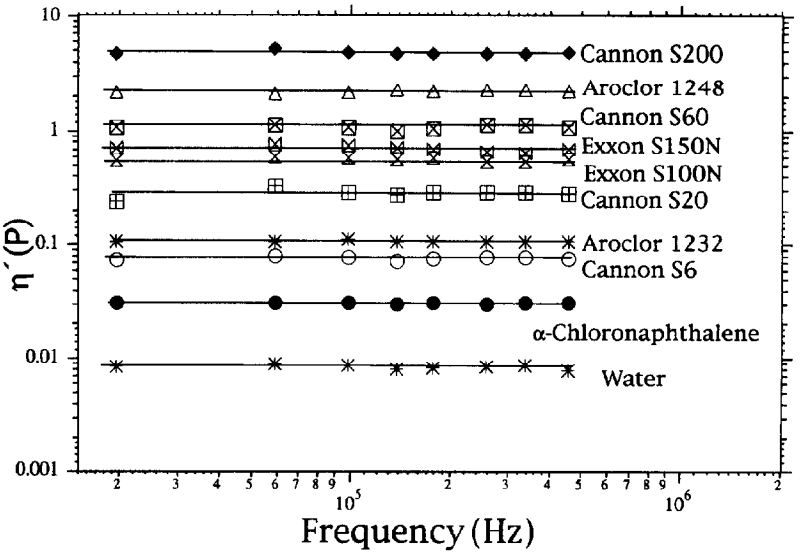

FIG. 7. Plots of η' vs frequency for a series of viscous liquids. Symbols are HFTRA data; the solid lines, known steady flow viscosities.

give rise to a complex propagating shear wave field; however, this contribution is independent of h and thus is effectively eliminated by the measurement and analysis methods employed. However, for *small* h, deviations in plots of $\Delta(1/\tau)_n$ and $\Delta\omega_{en}$ vs h from the predicted behavior are seen (see Fig. 4). Data in this region are discarded. Surface waves and surface viscoelastic properties associated with the upper liquid surface are also potential complications. These surface contributions, if significant, will lead to variations in the h dependence, different from that given in Eq. (8); this difference would be detectable only for the lowest mode. (Note that it may be possible to determine such surface properties with this type of transducer by employing a different analysis procedure and keeping h small.)

The measured eigenfrequency, damping coefficient, and fluid height are entered into a computer. For a given h, data is taken for each of the eight modes normally employed. Fluid height is then increased, and the entire process repeated for each of 15–20 fluid heights. Typical results are illustrated in Fig. 4 (115 000 MW polyisoprene in cis-decalin, $C = 0.100$ g/cm^3, $T = 25.00$ °C).

IV. EXPERIMENTAL RESULTS

The first step in evaluating this instrument was to run a series of Newtonian liquids ($\eta'' \cong 0$) of known viscosity [Radtke (1986)]. The results for this series of liquids are presented in Fig. 7; only values for η' are shown. (The small η'' values obtained were randomly scattered about zero, as expected.) The lines are the reported values of the low shear rate, steady flow viscosity for these liquids, which compare very well with the values obtained here.

Figure 8 compares the VE properties for solutions of 53 700 MW atactic polystyrene ($Mw/Mn = 1.02$) measured by three different instruments designed for dilute solution measurements. Two solutions were employed; Aroclor 1248 was the solvent for studies with the modified Birnboim apparatus (MBA), while Aroclor 1232 was used as the

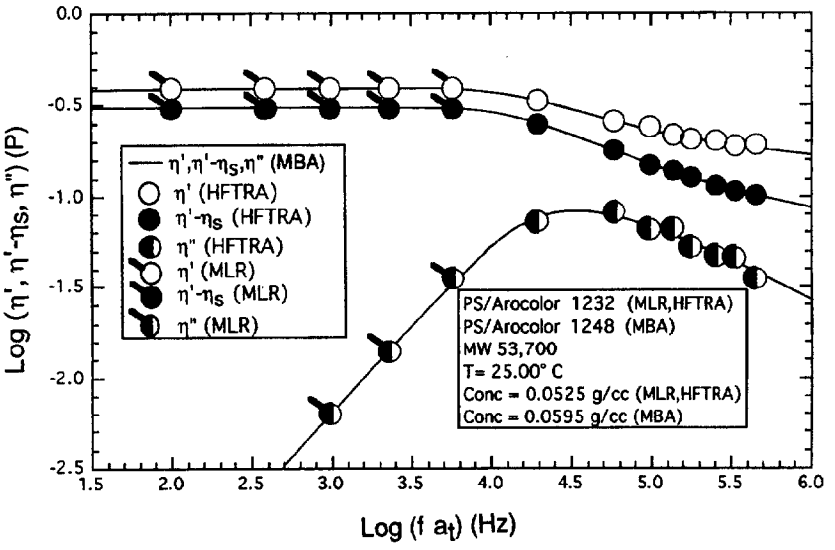

FIG. 8. The plot of viscoelastic properties versus frequency for a narrow distribution polystyrene in Aroclors measured with three different instruments. MLR data: circles with pips; HFTRA data: circles; MBA data: solid lines representing data taken at several different temperatures and time–temperature superposed to 25.00 °C, then corrected for differences in concentration and solvent viscosity (see the text).

solvent for measurements with the multiple lumped resonator (MLR) and high frequency torsional rod apparatus (HFTRA). (Previous studies in our group and others have shown that these two Aroclors exhibit nearly identical solvation conditions for polystyrene for temperatures near 25 °C.) The individual data points from the MLR (circles with pips) and HFTRA (circles) are shown; the solid lines represent the very large number of data points obtained with the MBA. Data for different temperatures obtained with the MBA were time/temperature superposed to 25.00 °C, the temperature employed for MLR and HFTRA measurements, and then shifted again to reflect the differences in solvent viscosity for Aroclor 1232 and Aroclor 1248 and a small difference in solution concentrations using the procedures of Landry [Landry (1985)] and Stokich [Stokich (1989)]. The agreement among the three instruments is excellent, illustrating the ability of the HFTRA to obtain precise results for dilute polymer solutions.

V. COMMENTS

The HFTRA provides adequate precision and a working frequency range suitable for moderately high-frequency viscoelastic studies of dilute polymer solutions employing low viscosity solvents; the frequency range is such that most of the relaxation time spectrum can be probed for many polymer/solvent combinations. There are instruments with higher precision, such as the MLR, and instruments capable of operating at higher frequencies, but this appears to be the first instrument capable of operating at these frequencies with the precision requisite for measurements of η' and η'' for dilute solutions. The use of a discrete set of frequencies is a limitation, but the present resonator provides reasonable coverage of the 20–500 kHz frequency range. The key feature of this apparatus is the method for precise measurements of the damping coefficient and eigenfrequency, particularly the former. The instrument is suitable for solutions for which

$0.003P < |\eta^*| < 5P$ if $\eta' \geq 1.33\eta''$. The lower limit on $|\eta^*|$ is set by inherent noise (electrical and mechanical), and the upper limit by the need to have surface loading conditions. Generally, η' has a relative uncertainty of 2% or less, with the η'' relative uncertainty being about 4% for solutions for which η'' is greater than $0.01P$.

ACKNOWLEDGMENTS

The authors would like to thank Dr. Crain and Dr. Strand for providing the MBA and MLR data, and the machine shop of the Department of Chemistry, in particular, Robert Schmelzer, for assistance in assembling this apparatus. Support was provided by the National Science Foundation Polymers Program through Grant Nos. DMR-8303207, DMR-8800641, and DMR-9223212.

References

Barlow, A. J. and J. Lamb, Proc. R. Soc. London Ser. A **298**, 52 (1959).

Blom, C. and J. Mellema, "Torsional Pendula with Electromagnetic Drive and Detection System for Measuring the Complex Shear Modulus of Liquids in the Frequency Range 80–2500 Hz,"Rheol. Acta **23**, 98–105 (1984).

Cooke, B. J. and A. J. Matheson, "Dynamic Viscosity of Dilute Polymer Solutions at High Frequencies of Alternating Shear Stress," J. Chem. Soc.**72**, 679 (1976).

Ellingsrud, S., K. D. Knudsen, A. Mikkelsen, A. Elgsaeter, and J. T. Malmo, "Torsional Dynamics of the Birnbiom–Schrag Multiple Lump Resonator Studied Using TV Holography," Rheol. Acta **31**, 459–470 (1992).

Ferry, J. D., *Viscoelastic Properties of Polymers* (Wiley, New York, 1980).

Glover, G. M., G. Hall, A. J. Matheson, and J. L. Stretton, J. Phys. E Sci. Instrum. **1**, 383 (1968).

Glover, G. M., G. Hall, A. J. Matheson, and J. L. Stretton, Proc. 5th Int. Congr. Rheol. **1**, 429 (1969).

Hair, D. W. and E. J. Amis, "Intrinsic Dynamic Viscoelasticity of Polystyrene in Theta and Good Solvents," Macromolecules **22**, 4528–4536 (1989).

Hair, D. W., F. J. Niertit, D. F. Hodgson, and E. J. Amis, "High Speed Averager for Characterizing Periodic Signals in the Time Domain," Rev. Sci. Instrum. **60**, 2780–2784 (1989).

Hunston, D. L., Ph.D. dissertation, Kent State University, 1969.

Hunston, D. L., R. R. Myers, and M. B. Palmer, Trans. Soc. Rheol. **16**, 33 (1972).

Koh, I. Y., "An Ultrasonic Method for Measurement of Viscoelastic Properties of Polymeric Solutions," Ph.D. dissertation, Rensselaer Polytechnic Institute, 1977.

Landry, C. J. T., "Effects of Concentration and Solvent on the Conformational Dynamics of Polystyrene Solutions as Revealed by Oscillatory Flow Birefringence," Ph.D. dissertation, University of Wisconsin-Madison, 1985.

Mason, W. P., W. O. Baker, J. H. McSkimin, and J. H. Heiss, Phys. Rev. **75**, 936 (1949).

Mason, W. P. and J. N. M. Hill, "Measurement of the Viscosity and Shear Elasticity of Liquids by Means of a Torsionally Vibrating Crystal," Trans. ASME **69**, 359–368 (1947).

McSkimin, H. J., "Measurement of Dynamic Shear Viscosity and Stiffness of Viscous Liquids by Means of Traveling Torsional Waves," J. Acoust. Soc. Am. **24**, 355–365 (1952).

Meeker, T. R. and A. H. Meitzler, "Guided Wave Propagation in Elongated Cylinders and Plates," in *Physical Acoustics*, edited by W. P. Mason (Academic, New York, 1964), , Vol. 1A, pp. 112–166.

Mikkelsen, A., K. D. Knudsen, and A. Elgsaeter, "Measurement of the Dynamic Viscoelastic Properties of Polymer Solutions Using the Birnbiom–Schrag Multiple Lump Resonator-A Theoretical and Numerical Study," Rheol. Acta **31**, 440–458 (1992).

Nakajima, H., H. Okamoto, and Y. Wada, "An Improved Apparatus for Measuring Complex Viscosity of Dilute Polymer Solutions at Frequencies from 2 to 500 kHz," Polym. J. **5**, 268 (1973).

Nakajima, H. and Y. Wada, "New Techniques for Measuring Complex Shear Viscosity of Dilute Polymer Solutions at Frequencies from 2 to 300 kHz," Polym. J. **1**, 727 (1970).

Ookubo, N., M. Komatsubara, H. Nakajima, and Y. Wada, "Infinite Dilution Viscoelastic Properties of Poly(*g*-benzyl-*l*-glutamate) in *m*-Cresol," Biopolymers **15**, 929–947 (1976).

Oosterbroek, M., H. A. Waterman, S. S. Wiseall, E. G. Altena, J. Mellema, and G. A. M. Kip, "Automatic Apparatus, Based Upon a Nickel-Tube Resonator, for Measuring the Complex Shear Modulus of Liquids in the kHz Range," Rheol. Acta **19**, 497–506 (1980).

Radtke, D. R., High Frequency Viscoelastic Properties of Polymer Solutions, Ph.D. dissertation, University of Wisconsin, 1986.

Sammler, R. L., C. J. Landry, G. R. Woltman, and J. L. Schrag, "Polydispersity Effects on Dilute-Solution Dynamic Properties of Linear Homopolymers," Macromolecules **23**, 2388–2396 (1990).

Schrag, J. L. and J. D. Ferry, "Mechanical Techniques for Studying Viscoelastic Relaxation Processes in Polymer Solutions," Faraday Symp.Chem. Soc. **6**, 182–193 (1972).

Schrag, J. L. and R. M. Johnson,"Application of the Birnboim Multiple Lumped Resonator Principle to Viscoelastic Measurements of Dilute Macromolecular Solutions," Rev. Sci. Instrum. **42**, 224–232 (1971).

Sittel, K., P. E. Rouse, and E. D. Bailey, "Method of Determining the Viscoelastic Properties of Dilute Polymer Solutions at Audio Frequencies," J. Appl. Phys. **25**, 1312–1320 (1954).

Stokich, T. M., "The Influence of Polymer/Solvent Interactions on the Viscoelastic and Oscillatory Flow Birefringence Properties of Polystyrene and Polyisoprene Solutions," Ph.D. dissertation, University of Wisconsin-Madison, 1989.

Tanaka, H., A. Sakanishi, and J. Furuichi, Zario **15**, 438 (1966).

Yoshizaki, H., "Measurement of Viscoelastic Properties of Polymer Solutions by Torsional Crystals," Polym. J. **25**, 553–559 (1993).